Journal of Systems Engineering and Electronics
Vol. 33, No. 4, August 2022, pp.877 – 886

Energy-efficient resource management for CCFD massive MIMO systems in 6G networks

SU Yumeng, GAO Hongyuan*, and ZHANG Shibo

College of Information and Communication Engineering, Harbin Engineering University, Harbin 150001, China

Abstract: This paper presents a co-time co-frequency full-duplex (CCFD) massive multiple-input multiple-output (MIMO) system to meet high spectrum efficiency requirements for beyond the fifth-generation (5G) and the forthcoming the sixth-generation (6G) networks. To achieve equilibrium of energy consumption, system resource utilization, and overall transmission capacity, an energy-efficient resource management strategy concerning power allocation and antenna selection is designed. A continuous quantum-inspired termite colony optimization (CQTCO) algorithm is proposed as a solution to the resource management considering the communication reliability while promoting energy conservation for the CCFD massive MIMO system. The effectiveness of CQTCO compared with other algorithms is evaluated through simulations. The results reveal that the proposed resource management scheme under CQTCO can obtain a superior performance in different communication scenarios, which can be considered as an eco-friendly solution for promoting reliable and efficient communication in future wireless networks.

Keywords: the sixth-generation (6G), massive multiple-input multiple-output (MIMO), co-time co-frequency full-duplex, energy-efficient, resource management.

DOI: 10.23919/JSEE.2022.000085

1. Introduction

With the growing popularity of smart devices and the coming era of Internet of Everything (IoE), wireless communication is becoming a strong propulsion for social transformation in present days [1]. To confront with the challenge of tremendous amount of data, the sixth-generation (6G) network is expected to realize wider coverage, ultra-high speed, and more stable transmissions in the near future [2–4]. However, with the booming development of information and communications technology (ICT), the percentage of global carbon emission is rapidly increasing [5–7]. This situation will escalate with the completion of the fifth-generation (5G) communication system. By 2026, the contamination caused by wireless communication will increase by 150% [8]. Nowadays, energy efficiency has become an important concern that should not be neglected while improving the transmission capacity. The awareness of energy conservation motivates researchers to carry out numerous studies for promoting green communication [7–9].

By exploiting large number of antennas, massive multiple-input multiple-output (MIMO) can achieve higher diversity gain and simultaneously serve many IoE devices, which is regarded as an effective solution to improve the system spectral efficiency and energy efficiency [10–15]. This promising technique has brilliant prospects owing to its simple, coherent processing methods, and good economic performance [16]. However, high energy cost is a critical challenge in massive MIMO networks due to the dense antennas at the base station (BS) [17]. Since most of the energy is consumed by the data center at the BS, antenna selection is an effective way to reduce the number of radio frequency chains and energy cost [18–20]. By traversing all antenna subsets, the antenna selection scheme with the best system performance can be performed by the exhaustive search method. However, the implementation cost is too high in massive MIMO systems with large-scale antennas. For alternative solutions, a suboptimal selection strategy based on iterative swapping was investigated in [21]. The authors in [22] considered a successive removal strategy by eliminating antennas with less influence on transmission capacity according to the channel state information (CSI) required from the previous user. As a complementary solution for improving the energy efficiency, power allo-

Manuscript received October 19, 2020.
*Corresponding author.
This work was supported by the Ph.D. Student Research and Innovation Fund of the Fundamental Research Funds for the Central Universities (3072020GIP0803), Heilongjiang Province Key Laboratory Fund of High Accuracy Satellite Navigation and Marine Application Laboratory (HKL-2020-Y01), the National Natural Science Foundation of China (61571149), the Initiation Fund for Postdoctoral Research in Heilongjiang Province (LBH-Q19098), and the Key Laboratory of Advanced Marine Communication and Information Technology, Ministry of Industry and Information Technology.

cation can effectively eliminate the near-far effect due to the differences of CSI among the users [23–25]. For most power allocation strategies, the main mathematical tool is based on the fractional programming optimization theory. However, this powerful tool fails in the presence of multi-user interference, which is difficult to extend to complicated communication scenarios.

Massive MIMO technology is originally investigated in a time-division duplex (TDD) operation system, while the BS and mobile stations must be coordinated with each other [10]. To improve the transmission efficiency of massive MIMO systems, many scholars have conducted in-depth researches on the implementation of frequency-division duplex (FDD) operation [26–28]. For TDD and FDD modes, the uplink and downlink transmissions are allocated to separate time slots or independent frequency bands, which is difficult to face the challenge of increasing shortage of time-frequency resources. Co-time co-frequency full-duplex (CCFD) technology enables simultaneous information transmission of both directions in the same frequency band [29]. Although this promising technology is attractive in high spectral efficiency, the implementation of CCFD is challenging due to the negative effect of strong self-interference [30]. In recent years, many self-interference elimination strategies based on independent component analysis, spatial suppression, and beamforming technologies were proposed to alleviate the negative influence on system performance [30–32]. In [33], Xia et al. investigated the technical feasibility of simultaneous uplink and downlink transmissions under the same frequency resources by beam-domain full-duplex operation. A higher spectral efficiency gain can be obtained compared to traditional TDD and FDD systems. However, the trade-off between the spectral efficiency and energy efficiency is not well achieved, while the performance is more inclined to equilibrium in 6G networks.

In order to address the aforementioned challenges and improve the overall performance, this paper proposes a macro-cell CCFD massive MIMO system under the reality circumstance of limited time-frequency resources. In this system, the BS and the users simultaneously transmit and receive information in one spectrum resource block. An energy-efficient resource management scheme is presented to achieve the trade-off between the transmission capacity, communication quality, and energy conservation. To this end, a hybrid resource management problem of uplink and downlink power allocation and antenna selection is formulated for the proposed CCFD massive MIMO system. Then, a continuous quantum-inspired termite colony optimization (CQTCO) algorithm is designed to find the best solution. The major contributions of this work are summarized as follows:

(i) A CCFD massive MIMO system is proposed to meet the challenge of limited time-frequency resources in practical communication networks. An energy-efficient resource management scheme concerning power allocation and antenna selection is proposed to promote reliable and efficient communication in line with green objectives.

(ii) Two important concerns on transmission capacity and energy efficiency are investigated in CCFD massive MIMO networks. Exact expressions are derived considering the equilibrium of energy consumption, requirement of users, and the transmission reliability for the communication system.

(iii) A CQTCO algorithm is proposed for the implementation of resource management in CCFD massive MIMO networks. Simulation results highlight the efficiency and excellent performance of CQTCO over traditional algorithms and strategies for multi-constraint non-convex optimization problems.

The rest of this paper is systemized as follows: The system model and mathematical expressions of transmission capacity and energy efficiency in CCFD massive MIMO networks are presented in Section 2. The principle of the CQTCO algorithm, the complexity analysis, and the process of resource management under CQTCO are introduced in Section 3. Simulation results and conclusions are presented in Section 4 and Section 5, respectively.

2. System model and analysis

2.1 System model

Consider a CCFD massive MIMO system that has an M-antenna BS and shares the same spectrum resource block with K legitimate users. The BS allocates M_t antennas to broadcast its information with the transmission power of $P_{\rm BS}$, while the remaining M_r antennas are used for receiving. Both large-scale and small-scale fading factors are included regarding the propagation channel of CCFD massive MIMO system [12]. Assume that the global CSI is available from legitimate devices and the CSI remains unchanged in one time slot [14,34,35]. The CSI vector from the uplink user k ($k=1,2,\cdots,K$) to the receiving antennas of the BS is denoted as $\boldsymbol{G}_{u_k\_{\rm BS}} \in \mathbb{C}^{M_r\times 1}$, and the CSI vector from the downlink transmitting antennas of the BS to the kth user is denoted as $\boldsymbol{G}_{{\rm BS}\_u_k} \in \mathbb{C}^{1\times M_t}$. The self-interference channel matrix of the BS is denoted as $\boldsymbol{G}^I_{\rm BS} \in \mathbb{C}^{M_r\times M_t}$. The self-interference channel of the kth user is denoted as $G^I_{u_k}$, and the interference channel between the kth user and the jth ($j=1,2,\cdots,K,\ j\neq k$) user is denoted as $G^I_{u_{k,j}}$. Maximum ratio transmission (MRT) and maximum ratio combining (MRC) are employed for precoding and receiving at the BS.

Since the BS simultaneously transmits and receives signals in the same frequency band, it generates self-interference. The same goes for the users. For practical implementation, assume that transmitting and receiving antennas of each user are deployed on different sides of the equipment. The degree of self-interference cancellation (SIC) is qualified by $\rho \in [0,1]$, where $\rho = 0$ denotes zero self-interference [34]. The receiving signals at the BS and the kth user are respectively given by

$$\boldsymbol{y}_{\mathrm{BS}} = \sqrt{\rho_{\mathrm{BS}} P_{\mathrm{BS}}} \boldsymbol{W}^{\mathrm{H}} \boldsymbol{G}_{\mathrm{BS}}^{I} \boldsymbol{V} \boldsymbol{s}_{\mathrm{BS}} + \sum_{k=1}^{K} \sqrt{P_k} \boldsymbol{W}^{\mathrm{H}} \boldsymbol{G}_{u_k\_\mathrm{BS}} \boldsymbol{s}_k + \boldsymbol{n}_{\mathrm{BS}} \tag{1}$$

and

$$\begin{aligned} \boldsymbol{y}_k = {} & \sqrt{P_{\mathrm{BS}}} \boldsymbol{G}_{\mathrm{BS}\_u_k} \boldsymbol{V} \boldsymbol{s}_{\mathrm{BS}} + \sqrt{\rho_u P_k} G_{u_k}^{I} \boldsymbol{s}_k + \\ & \sum_{j=1, j\neq k}^{K} \sqrt{P_j} G_{u_{k,j}}^{I} \boldsymbol{s}_j + \boldsymbol{n}_k \end{aligned} \tag{2}$$

where ρ_{BS} and ρ_u denote the self-interference levels at the BS and the users respectively; P_k and P_j are transmission power of the kth user and the jth user respectively; $\boldsymbol{s}_{\mathrm{BS}}$, $\boldsymbol{s}_k$, and $\boldsymbol{s}_j$ are complex Gaussian signals transmitted by the BS, user k, and user j, with $\mathrm{E}\{\|\boldsymbol{s}_{\mathrm{BS}}\|^2\} = 1$, $\mathrm{E}\{\|\boldsymbol{s}_k\|^2\} = 1$, and $\mathrm{E}\{\|\boldsymbol{s}_j\|^2\} = 1$, respectively. $\boldsymbol{W} \in \mathbb{C}^{M_r \times K}$ ($\boldsymbol{W} = [\boldsymbol{w}_1, \boldsymbol{w}_2, \cdots, \boldsymbol{w}_K]$) and $\boldsymbol{V} \in \mathbb{C}^{M_t \times K}$ ($\boldsymbol{V} = [\boldsymbol{v}_1, \boldsymbol{v}_2, \cdots, \boldsymbol{v}_K]$) represent the receiving matrix and the precoding matrix at the BS respectively. According to the MRC/MRT criterion [12,35], the receiving vector and the precoding vector of the BS to user k can be expressed by $\boldsymbol{w}_k = \boldsymbol{G}_{u_k\_\mathrm{BS}} / \|\boldsymbol{G}_{u_k\_\mathrm{BS}}\|$ and $\boldsymbol{v}_k = \boldsymbol{G}_{\mathrm{BS}\_u_k}^{\mathrm{H}} / \|\boldsymbol{G}_{\mathrm{BS}\_u_k}\|$, respectively. $\boldsymbol{n}_{\mathrm{BS}}$ and $\boldsymbol{n}_k$ are additive white Gaussian noise (AWGN) at the BS and the kth user.

The uplink signal-to-interference-plus-noise ratio (SINR) received at the BS from the kth user is given by

$$\gamma_k = \frac{P_k \|\boldsymbol{W}^{\mathrm{H}} \boldsymbol{G}_{u_k\_\mathrm{BS}}\|^2}{\rho_{\mathrm{BS}} P_{\mathrm{BS}} \|\boldsymbol{W}^{\mathrm{H}} \boldsymbol{G}_{\mathrm{BS}}^{I} \boldsymbol{V}\|^2 + \sum\limits_{j=1, j\neq k}^{K} P_j \|\boldsymbol{W}^{\mathrm{H}} \boldsymbol{G}_{u_j\_\mathrm{BS}}\|^2 + \sigma_{\mathrm{BS}}^2} \tag{3}$$

where σ_{BS}^2 denotes the AWGN power at the BS. For uplink transmission, the transmission rate from the kth user can be calculated as

$$R_k = B \log_2(1 + \gamma_k) \tag{4}$$

where B denotes the frequency bandwidth. Then, the uplink transmission rate of CCFD massive MIMO networks can be calculated as

$$R = \sum_{k=1}^{K} R_k = \sum_{k=1}^{K} B \log_2(1 + \gamma_k). \tag{5}$$

For downlink transmission, the SINR received at the kth user from the BS is denoted as

$$\gamma_k' = \frac{P_{\mathrm{BS}} |\boldsymbol{G}_{\mathrm{BS}\_u_k} \boldsymbol{v}_k|^2}{\rho_u P_k |G_{u_k}^{I}|^2 + \sum\limits_{j=1, j\neq k}^{K} P_{\mathrm{BS}} |\boldsymbol{G}_{\mathrm{BS}\_u_k} \boldsymbol{v}_j|^2 + \sum\limits_{j=1, j\neq k}^{K} P_j |G_{u_{k,j}}^{I}|^2 + \sigma_k^2} \tag{6}$$

where σ_k^2 is the AWGN power received by the kth user. The downlink transmission rate from the BS to the kth user can be calculated by

$$R_k' = B \log_2(1 + \gamma_k'). \tag{7}$$

Accordingly, the downlink transmission rate of CCFD massive MIMO networks can be shown by

$$R' = \sum_{k=1}^{K} R'_k = \sum_{k=1}^{K} B \log_2(1 + \gamma'_k). \tag{8}$$

2.2 Transmission capacity and energy efficiency

Typically, the transmission capacity of a full-duplex system is calculated by the sum rate of uplink/downlink transmissions. However, the total transmission rate may not necessarily reflect the overall performance of CCFD massive MIMO networks, since the uplink and downlink transmission rates are difficult to be determined. This motivates our definition of overall transmission capacity in CCFD massive MIMO networks, which is given by

$$C = \min\,(R, R') \tag{9}$$

where R and R' are respectively given by (5) and (8).

The energy efficiency is characterized by the ratio of transmission capacity to the power consumption of the system. The power consumed in this system [8,24,36] can be calculated by

$$P_{\mathrm{total}} = P_c + \frac{1}{\eta}\left(\sum_{k=1}^{K} P_k + M_t P_{\mathrm{BS}}\right) \tag{10}$$

where P_c denotes the power consumption on system circuit, and η denotes the energy conversion efficiency. The energy efficiency of CCFD massive MIMO networks can be calculated by

$$\varphi = \frac{C}{P_{\mathrm{total}}} = \frac{\min\,(R, R')}{P_{\mathrm{total}}}. \tag{11}$$

2.3 Problem formulation

Considering the resource management strategy includes uplink power allocation and antenna selection in CCFD massive MIMO networks, the problem for the overall transmission capacity optimization is shown as

$$\max\ C(M_t,\boldsymbol{P}) = \max\{\min[R(M_t,\boldsymbol{P}), R'(M_t,\boldsymbol{P})]\}$$
$$\text{s.t.}\begin{cases}0 \leqslant P_k \leqslant P_k^{\max},\ k=1,2,\cdots,K\\ 0 < M_t < M\end{cases} \tag{12}$$

where $\boldsymbol{P} = [P_1, P_2, \cdots, P_K]$ is the feasible set of transmission power of users, $P_k^{\max}$ is the maximum transmission power of the kth user.

Transmission capacity and energy efficiency are two major concerns in massive MIMO networks, while these issues are conflicting to some extent. In order to achieve the maximum energy efficiency on the premise of guaranteeing transmission requirements of legitimate devices in CCFD massive MIMO networks, the optimization problem can be expressed as

$$\max\ \varphi(M_t,\boldsymbol{P}) = \max\left\{\frac{\min[R(M_t,\boldsymbol{P}), R'(M_t,\boldsymbol{P})]}{P_{\text{total}}(M_t,\boldsymbol{P})}\right\}$$
$$\text{s.t.}\begin{cases}0 \leqslant P_k \leqslant P_k^{\max},\ k=1,2,\cdots,K\\ 0 < M_t < M\\ R \geqslant R_{\min}\\ R' \geqslant R'_{\min}\end{cases} \tag{13}$$

where $R_{\min}$ and $R'_{\min}$ denote the required minimum uplink and downlink transmission rates respectively.

As shown in (12) and (13), the maximizations for overall transmission capacity and energy efficiency are non-convex optimization problems which are non-deterministic polynominal-hard (NP-hard) for traditional mathematical techniques and algorithms to find the appropriate solution. Therefore, an efficient intelligent algorithm is proposed to tackle the complicated optimization problems.

3. Energy-efficient resource management based on CQTCO

3.1 CQTCO algorithm

The CQTCO algorithm that combines the advantages of the termite colony optimization (TCO) mechanism [37] and quantum intelligence computation [38] is proposed in this section. The CQTCO algorithm employs a colony of H quantum termites searching in a D-dimensional space, where D represents the maximal dimension of the optimization problem.

In CQTCO, a quantum termite is made up by D quantum bits. The ith $(i = 1,2,\cdots,H)$ quantum termite of the tth iteration is given by

$$\boldsymbol{x}_i^t = \begin{bmatrix}\alpha_{i,1}^t, \alpha_{i,2}^t, \cdots, \alpha_{i,D}^t\\ \beta_{i,1}^t, \beta_{i,2}^t, \cdots, \beta_{i,D}^t\end{bmatrix} \tag{14}$$

where $\left[\alpha_{i,d}^t, \beta_{i,d}^t\right]^{\mathrm{T}}$ denotes the dth $(d = 1,2,\cdots,D)$ quantum bit of the ith quantum termite, $|\alpha_{i,d}^t|^2 + |\beta_{i,d}^t|^2 = 1$, $0 \leqslant \alpha_{i,d}^t \leqslant 1$, and $0 \leqslant \beta_{i,d}^t \leqslant 1$. Then, $\beta_{i,d}^t = \sqrt{1-(\alpha_{i,d}^t)^2}$. To enhance the efficiency of CQTCO, the ith quantum termite can be simplified by

$$\boldsymbol{x}_i^t = [\alpha_{i,1}^t, \alpha_{i,2}^t, \cdots, \alpha_{i,D}^t] = [x_{i,1}^t, x_{i,2}^t, \cdots, x_{i,D}^t] \tag{15}$$

where $0 \leqslant x_{i,d}^t \leqslant 1$ $(d = 1,2,\cdots,D)$, and $x_{i,d}^t$ denotes the simplified dth quantum bit of the quantum termite i. The position of the ith quantum termite is obtained by

$$\bar{x}_{i,d}^t = \bar{x}_{i,d}^{\min} + (\bar{x}_{i,d}^{\max} - \bar{x}_{i,d}^{\min})\cdot x_{i,d}^t \tag{16}$$

where $\bar{x}_{i,d}^t$ denotes the dth position of the ith quantum termite, and $\bar{x}_{i,d}^{\max}$ and $\bar{x}_{i,d}^{\min}$ denote the dth upper bound and lower bound of the searching range respectively. The position of each quantum termite is corresponding to a feasible solution for the optimization problem.

The fitness value of the ith quantum termite is expressed as $f(\bar{\boldsymbol{x}}_i^t)$, where $f(\cdot)$ denotes the fitness function. The position of each quantum termite i with the best fitness value is defined as the local optimal position, $\bar{\boldsymbol{p}}_i^t = [\bar{p}_{i,1}^t, \bar{p}_{i,2}^t, \cdots, \bar{p}_{i,D}^t]$. The position of the quantum termite with the best fitness value is defined as the global optimal position, $\bar{\boldsymbol{p}}_g^t = [\bar{p}_{g,1}^t, \bar{p}_{g,2}^t, \cdots, \bar{p}_{g,D}^t]$.

The evolution of each quantum termite is based on quantum rotation angle and pheromone contents at the positions of quantum termites. In each iteration process of the quantum termite colony, the pheromone content at the position of each quantum termite is updated by

$$\mu_i^{t+1} = \frac{(1-e)\mu_i^t + 1}{1+\exp(-f(\bar{\boldsymbol{x}}_i^t))} \tag{17}$$

where e is the evaporation rate of the pheromone with $0 \leqslant e \leqslant 1$, and μ_i^t is the pheromone content of the ith quantum termite in the tth iteration. The initial pheromone content of each quantum termite is set to 0.

In CQTCO, each quantum termite adjusts its movement based on the information of the quantum termite colony and the pheromones of neighboring quantum termites. The neighborhood of a quantum termite i is determined by its search radius τ_i^t, and the set of its neighboring quantum termites is expressed as $\boldsymbol{Z}_i^{t+1}$. The position of the neighboring quantum termite with the highest pheromone is denoted as $\bar{\boldsymbol{v}}_i^t = [\bar{v}_{i,1}^t, \bar{v}_{i,2}^t, \cdots, \bar{v}_{i,D}^t]$. For quantum termite i, if neighboring quantum termite has higher pheromones, the quantum rotation angle is generated by

$$\theta_{i,d}^{t+1} = c_1(\bar{v}_{i,d}^t - \bar{x}_{i,d}^t) + c_2(\bar{p}_{g,d}^t - \bar{x}_{i,d}^t) \tag{18}$$

where $\theta_{i,d}^{t+1}$ represents the dth dimension of quantum rotation angle, c_1 is the impact factor of the best neighboring position, and c_2 is the impact factor of the global optimal position. Otherwise, the quantum rotation angle is generated by

$$\theta_{i,d}^{t+1} = c_3 \cdot \lambda_{i,d}^{t+1} \cdot (\bar{x}_{r,d}^t - \bar{x}_{i,d}^t) + c_4(\bar{p}_{i,d}^t - \bar{x}_{i,d}^t) \tag{19}$$

where c_3 is a constant related to the random walk; c_4 denotes the impact factor of the local optimal position; $\lambda_{i,d}^t$ is a random variable distributed in $[-1,1]$; $\bar{x}_{r,d}^t$ denotes the dth position of an arbitrary quantum termite, $r \in \{1,2,\cdots,H\}$, $r \neq i$.

The quantum bit of each quantum termite is generated by the following rules:

$$\omega_{i,d}^{t+1} = \begin{cases} \sqrt{1-(x_{i,d}^t)^2}, \ \theta_{i,d}^{t+1} = 0; \ \delta_{i,d}^{t+1} \leqslant c_5 \\ \text{abs}\,(x_{i,d}^t \cdot \cos\,\theta_{i,d}^{t+1} + \sqrt{1-(x_{i,d}^t)^2} \cdot \sin\,\theta_{i,d}^{t+1}), \quad \text{otherwise} \end{cases} \tag{20}$$

where $\delta_{i,d}^{t+1}$ denotes a random variable distributed in the range $[0,1]$, c_5 denotes the conversion probability, and $\text{abs}(\cdot)$ denotes the absolute value function.

The updated position $\bar{\boldsymbol{\omega}}_i^{t+1}$ can be obtained by (16). The fitness value of the updated quantum termites can be calculated by fitness function. If the fitness of $\bar{\boldsymbol{\omega}}_i^{t+1}$ is higher than $\bar{\boldsymbol{x}}_i^t$, $\boldsymbol{x}_i^{t+1} = \boldsymbol{\omega}_i^{t+1}$, $\bar{\boldsymbol{x}}_i^{t+1} = \bar{\boldsymbol{\omega}}_i^{t+1}$; otherwise, $\boldsymbol{x}_i^{t+1} = \boldsymbol{x}_i^t$, $\bar{\boldsymbol{x}}_i^{t+1} = \bar{\boldsymbol{x}}_i^t$. Then update the local optimal position and the global optimal position of CQTCO until the $(t+1)$th iteration.

The iteration process ends when the algorithm achieves the terminal condition, which is determined by the maximum iteration number $t_{\max}$.

3.2 Computational complexity analysis of CQTCO

As introduced in Subsection 3.1, each quantum termite needs to calculate its pheromone content and find out the highest pheromone content of its neighbors, with computational complexity of $O(2H)$, where H stands for the population size of quantum termites. Quantum termites are updated by quantum rotation angles as shown in (18) and (19), with computational complexity of $O(HD)$, where D represents the dimension of quantum termites. The quantum bits of each quantum termite can be obtained by (20), and the updated position can be obtained by (16), with computational complexity of $O(2HD)$. After these processes, the fitness value of each quantum termite is calculated, with the complexity of $O(H)$. Then, the position of each quantum termite, the local optimal position, and the global optimal position of the quantum termite colony are updated after each iteration, with the complexity of $O(2H)$.

For the termination of CQTCO after t iterations, the computational complexity is $O(t(5H+3HD))$.

3.3 Process of resource management based on CQTCO

According to (12) and (13), the number of transmitting antennas and the uplink transmission power of each user should be optimized to achieve the maximum transmission capacity and energy efficiency in CCFD massive MIMO networks. Since these parameters are discrete and continuous variables that belong to different optimization domains, the number of transmitting antennas can be expressed as $M_t = \lceil \xi \cdot M \rceil$ to facilitate the solution of the difficulty, where ξ stands for the antenna selection coefficient at the BS. Hence, the hybrid problems of (12) and (13) can be transformed to continuous optimization problems, and the dimension of each quantum termite in CQTCO is $D = (K+1)$. The position of a quantum termite is corresponding to a feasible antenna selection and power allocation result in CCFD massive MIMO networks, that is, $\bar{\boldsymbol{x}}_i^t = [\bar{x}_{i,1}^t, \bar{x}_{i,2}^t, \cdots, \bar{x}_{i,D}^t] = [\xi_i^t, P_{i,1}^t, P_{i,2}^t, \cdots, P_{i,K}^t]$. For the problem of transmission capacity maximization, the fitness function is set as

$$f(\bar{\boldsymbol{x}}_i^t) = \begin{cases} C(\bar{\boldsymbol{x}}_i^t), & \text{satisfy constraint conditions} \\ 0, & \text{otherwise} \end{cases}.$$

For energy efficiency optimization, the fitness function is set as

$$f(\bar{\boldsymbol{x}}_i^t) = \begin{cases} \varphi(\bar{\boldsymbol{x}}_i^t), & \text{constraint conditions satisfied} \\ 0, & \text{otherwise} \end{cases}.$$

The implementation process is shown in the following steps:

Step 1 Initialize parameter settings of CCFD massive MIMO system.

Step 2 Randomly generate the initial colony of H quantum termites based on quantum coding mechanism. Calculate the fitness value of each quantum termite and find the local optimal position and global optimal position of the pheromone colony.

Step 3 Calculate the pheromone content of each quantum termite and perform evolution process.

Step 4 Obtain the updated position of each quantum termite and calculate the fitness value. Update the quantum termite according to the greedy mechanism.

Step 5 Update the local optimal position and global optimal position of the pheromone colony.

Step 6 If the iteration does not achieve the predefined value of the maximum iteration number, go to Step 3. Otherwise, the iteration process ends.

Step 7 Obtain the corresponding resource management scheme according to the global optimal position of CQTCO.

4. Simulation results

In this section, the overall performance of the proposed resource management scheme is evaluated under the CQTCO algorithm. Consider a macro cell CCFD massive MIMO network where K legitimate users are randomly distributed in the coverage area of the BS. To make things easy, assume that the maximum transmission power of all users are same, $P_k^{\max} = P_{\max}$, $\forall k$, and the SIC degrees at the BS are the same of the users. The simulation parameters of the CCFD massive MIMO system are presented in Table 1. All results are the average of 200 Monte-Carlo simulations.

Table 1 Simulation parameters

Parameter	Value
Number of antennas at the BS	128
Number of users	10
Coverage of the BS/m	500
Path loss exponent	3.8
Reference distance/m	100
Energy conversion efficiency	0.5
Transmission power of the BS/dBm	35
Maximum transmission power of users/dBm	30
SIC level/dB	−20
Circuit power consumption/dBm	10
System bandwidth/MHz	10
Minimum uplink/downlink transmission rate/(Mbit·s^{-1})	1
Noise power spectral density/(dBm·Hz^{-1})	−174

4.1 Performance comparison of CQTCO

The performance comparisons of the proposed CQTCO with other algorithms and strategies are shown in this section. In fact, researches have shown that there are no algorithms or strategies specifically designed for complicated non-convex optimization problems. For comparison purpose, some classical intelligent algorithms including TCO [37], particle swarm optimization (PSO) [39], and backtracking search optimization (BSO) [40], and the half power-random resource allocation (HPRRA) in [38] are applied for the problem of transmission capacity and energy efficiency maximization in CCFD massive MIMO networks. For the HPRRA scheme, all users broadcast their information at half of the maximum transmission power while the BS adopts the random antenna selection criterion. The population size of QTCO, TCO, PSO, and BSO algorithms is 20, and the terminal iteration number of these algorithms is set to 500. For QTCO, the search radius of each quantum termite is linearly decreased from $\tau_{\max}$ to $\tau_{\min}$ throughout the iterations. Set $\tau_{\max} = 3$, $\tau_{\min} = 1$, $e = 0.8$, $c_1 = 0.03$, $c_2 = 0.03$, $c_3 = 0.06$, and $c_4 = 0.01$. The parameter settings of TCO, PSO, and BSO algorithms can refer to [37,39], and [40], respectively.

The convergence performance of TCO, PSO, BSO and the proposed CQTCO is shown in Fig. 1. The result illustrates that the proposed CQTCO has a fast convergence speed and can obtain a higher transmission capacity compared with other algorithms. Intelligence algorithms like PSO, TCO, and BSO are well-accepted for solving engineering problems. However, these algorithms are easy to fall into the local optimum, especially for complicated non-convex optimization problems. To overcome the shortcomings of traditional algorithms, the CQTCO algorithm combines the mechanism of TCO and the advantage of quantum intelligence computation. Under the guidance of quantum evolution strategies, the population diversity of the CQTCO is superior to traditional algorithms, and the quantum colony can quickly converge to the best solution via global information sharing. Therefore, the CQTCO algorithm has the ability to find the best resource management result and achieve the highest transmission capacity in CCFD massive MIMO networks.

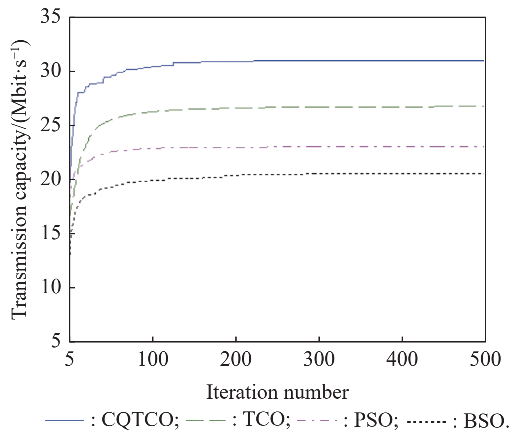

Fig. 1 Convergence performance comparison

Fig. 2 shows the transmission capacity comparison under CQTCO, TCO, PSO, BSO, and HPRRA schemes in different maximum transmission power of users, where $P_{\max}$ varies from 10 dBm to 30 dBm. Simulation results illustrate that the transmission capacity increases with $P_{\max}$. It is clear that a higher $P_{\max}$ may grant users more energy for information transmission, and the uplink user can achieve a higher transmission rate with larger transmission power. Hence, the transmission capacity is a monotonically increasing function of $P_{\max}$. Compared with other strategies, CQTCO can obtain the largest transmission capacity for any $P_{\max}$, especially when

P_{max} = 30 dBm, the transmission capacity of CQTCO is 14.8%, 34.8%, 47.6%, and nearly two times higher than that of the TCO, PCO, BSO, and HPRRA schemes.

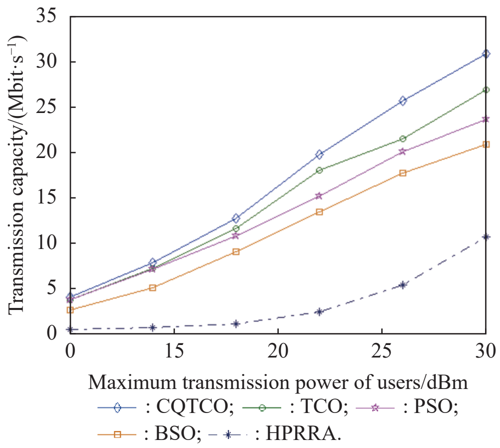

Fig. 2 Transmission capacity comparison with different P_{max}

Fig. 3 examines the energy efficiency performance under CQTCO, TCO, PSO, BSO, and HPRRA schemes with the variation of P_{max}. As presented in Subsection 2.2, energy efficiency is somewhat competitive with transmission capacity. When the users broadcast their signals with higher transmission power, the system will achieve a higher transmission capacity. However, energy efficiency is not a monotonically increasing function of transmission power and it will decrease when the increase of power consumption exceeds the increase of transmission capacity. As for CQTCO, the energy efficiency gradually increases with P_{max} at first, and then tends to be stable when P_{max} is over 22 dBm. As for TCO, PSO, and BSO, the energy efficiency of these schemes gradually increases with P_{max}, but they both experience a sharp decrease when P_{max} is over 24 dBm. Though TCO, PSO, and BSO algorithms can obtain larger transmission capacity with P_{max} as depicted in Fig. 2, the energy efficiency of these algorithms decrease in the case of higher P_{max}. As for HRPPA, although the energy efficiency increases with the maximum transmission power of users, the energy efficiency is the lowest among all schemes. Simulation results demonstrate the stability and reliability of CQTCO for solving the energy efficiency optimization problem with multi-constraints in (13). The results also conclude that CQTCO achieves the maximum energy efficiency in CCFD massive MIMO networks.

The influence of the self-interference level on the transmission capacity under CQTCO, TCO, PSO, BSO, and HPRRA schemes is investigated in Fig. 4. During the simulation, the self-interference level varies from −35 dB to −10 dB. For all strategies, transmission capacity is higher with smaller self-interference. The reason is that self-interference is harmful to the SINR received at legitimate devices as depicted in (3) and (6). Hence, the uplink/downlink transmission rate degrades as the increment of the self-interference level at the BS and the users. It is observed that CQTCO can achieve the best performance in different situations as depicted in Figs. 1−4. All results highlight the reliability of CQTCO compared with other strategies.

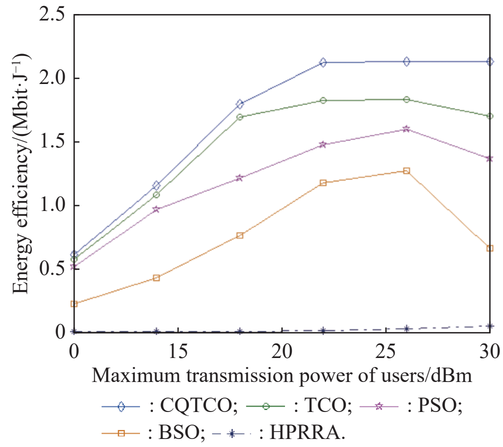

Fig. 3 Energy efficiency comparison with different P_{max}

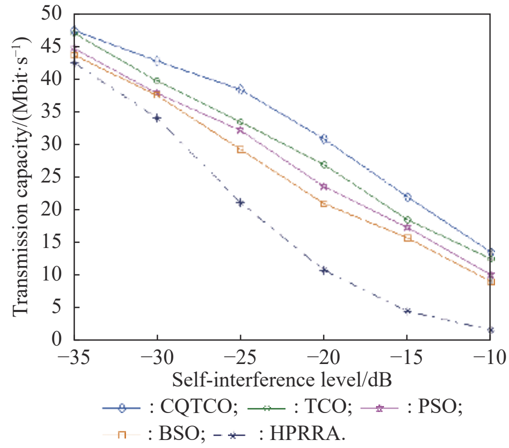

Fig. 4 Transmission capacity comparison with different self-interference level

4.2 Impact of different parameters

This subsection examines the transmission capacity and energy efficiency performance of the resource management scheme based on the CQTCO algorithm in different system parameters. The impact of transmission power, self-interference level, number of antennas, and users on the overall performance in CCFD massive MIMO networks are shown in the following.

Fig. 5 shows the energy efficiency performance with the variation of the self-interference level and transmission power of BS in CCFD massive MIMO networks. In the simulation, P_{BS} is equal to 20 dBm, 25 dBm, 30 dBm, and 35 dBm, and the self-interference level varies from −35 dB to −10 dB. Under these conditions, the energy efficiency gradually decreases with the increase of self-interference level. The result also illustrates that the system can achieve a higher energy efficiency in a smaller P_{BS} while guaranteeing the uplink/downlink transmission requirements. Hence, proper transmission power and smaller self-interference level is beneficial to achieve the communication reliability while promoting energy conservation.

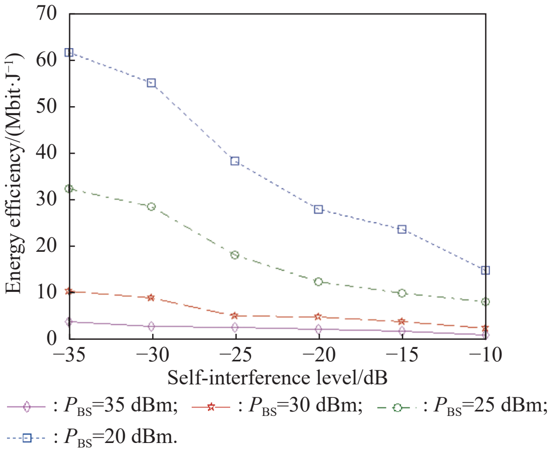

Fig. 5 Energy efficiency with different self-interference levels and P_{BS}

In Fig. 6, impacts of different numbers of users and antennas on the transmission capacity are investigated in CCFD massive MIMO networks where P_{max} varies from 10 dBm to 30 dBm with $K = 5$, $M = 64$, $K = 5$, $M = 128$, $K = 10$, $M = 64$, $K = 10$, $M = 128$. From the simulations, the transmission capacity increases with P_{max}, which is consistent with Fig. 2. The results also illustrates that the transmission capacity is higher where there is a larger number of users and antennas at the BS in the communication system.

Fig. 7 and Fig. 8 illustrate the transmission capacity and energy efficiency with different numbers of users and antennas in CCFD massive MIMO networks. The results of Fig. 7 show that the overall transmission capacity increases with a larger number of users. Also, a higher transmission capacity can be achieved where the BS is equipped with a larger number of antennas. However, as depicted in Fig. 8, energy efficiency shows an opposite trend compared with Fig. 7. The energy efficiency significantly decreases with the number of antennas and users. The reason is that denser nodes will bring more energy consumption in a communication system, and the increase of energy consumption is greater than that of the transmission rate. Therefore, it is necessary to reduce the network density to promote the balance between energy efficiency and transmission capacity in actual communication systems.

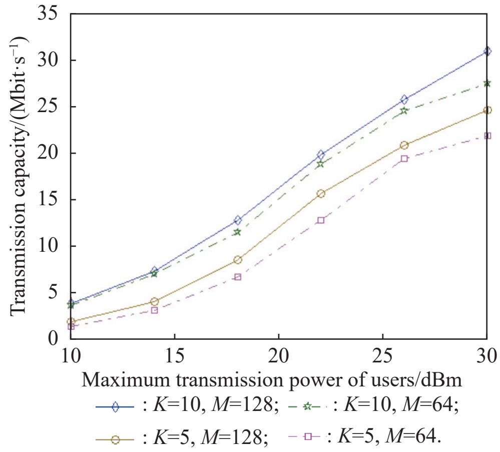

Fig. 6 Transmission capacity with different P_{max}, K, and M

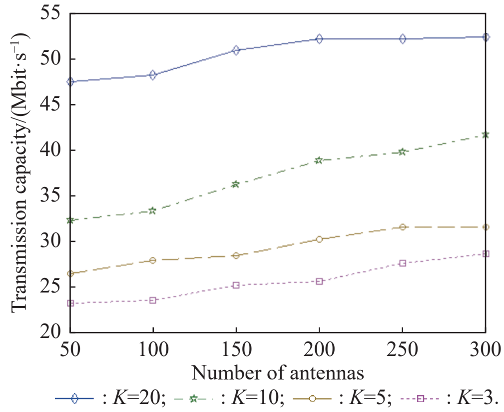

Fig. 7 Transmission capacity with different M and K

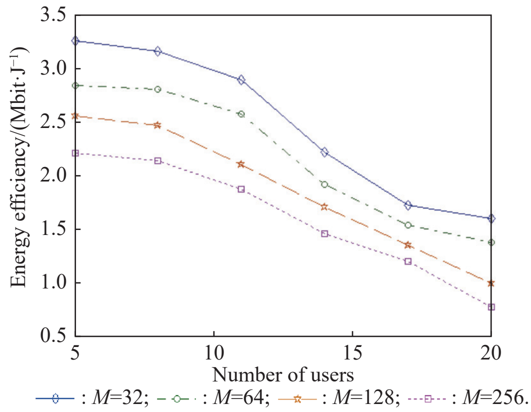

Fig. 8 Energy efficiency with different M and K

5. Conclusions

In this paper, the overall performance is investigated in

CCFD massive MIMO networks. Expressions for transmission capacity and energy efficiency are derived considering the transmission reliability of uplink and downlink transmissions. In order to achieve the high communication quality while promoting energy conservation, an energy-efficiency resource management scheme including power allocation and antenna selection is designed. Then, a CQTCO algorithm is proposed to obtain the best resource management scheme for the CCFD massive MIMO network. Simulation results highlight the merits of CQTCO over traditional algorithms and strategies in different system parameters. This work has provided an eco-friendly solution for the equilibrium of energy consumption, resource utilization, and transmission efficiency. It would be beneficial to extend the application of this work to multi-cell heterogeneous networks and ultra-dense scenarios toward future wireless cellular system.

References

[1] YAACOUB E, ALOUINI M S. A key 6G challenge and opportunity—connecting the base of the pyramid: a survey on rural connectivity. Proceedings of the IEEE, 2020, 108(4): 533–582.

[2] SAAD W, BENNIS M, CHEN M Z. A vision of 6G wireless systems: applications, trends, technologies, and open research problems. IEEE Network, 2020, 34(3): 134–142.

[3] SERGIOU C, LESTAS M, ANTONIOU P, et al. Complex systems: a communication networks perspective towards 6G. IEEE Access, 2020, 8: 89007–89030.

[4] ZHANG L, LIANG Y C, NIYATO D. 6G visions: mobile ultra-broadband, super Internet-of-Things, and artificial intelligence. China Communications, 2019, 16(8): 1–14.

[5] HUANG T Y, YANG W, WU J, et al. A survey on green 6G network: architecture and technologies. IEEE Access, 2019, 7: 175758–175768.

[6] DONG W, XU Z H, LI X X, et al. Low-cost subarrayed sensor array design strategy for IoT and future 6G applications. IEEE Internet of Things Journal, 2020, 7(6): 4816–4826.

[7] CHANG K C, CHU K C, WANG H C, et al. Energy saving technology of 5G base station based on Internet of Things collaborative control. IEEE Access, 2020, 8: 32935–32946.

[8] CHENG W G, ZHANG X, ZHANG H L. Statistical-QoS driven energy-efficiency optimization over green 5G mobile wireless networks. IEEE Journal on Selected Areas in Communications, 2016, 34(12): 3092–3107.

[9] QI Q, CHEN X M, ZHONG C T, et al. Integration of energy, computation and communication in 6G cellular Internet of Things. IEEE Communications Letters, 2020, 24(6): 1333–1337.

[10] MARZETTA T L. Noncooperative cellular wireless with unlimited numbers of base station antennas. IEEE Trans. on Wireless Communications, 2010, 9(11): 3590–3600.

[11] LV T J, LIN Z P, HUANG P M, et al. Optimization of the energy-efficient relay-based massive IoT network. IEEE Internet of Things Journal, 2018, 5(4): 3043–3058.

[12] HOANG T M, DUONG T Q, TUAN H D, et al. Secure massive MIMO relaying systems in a Poisson field of eavesdroppers. IEEE Trans. on Communications, 2017, 65(11): 4857–4870.

[13] LIU Y, WANG C X, HUANG J, et al. Novel 3-D nonstationary mmwave massive MIMO channel models for 5G high-speed train wireless communications. IEEE Trans. on Vehicular Technology, 2019, 68(3): 2077–2086.

[14] RAWAT D B, WHITE T, PARWEZ M S, et al. Evaluating secrecy outage of physical layer security in large-scale MIMO wireless communications for cyber-physical systems. IEEE Internet of Things Journal, 2017, 4(6): 1987–1993.

[15] HUANG B, GUO A H. Spectral and energy efficient resource allocation for massive MIMO HetNets with wireless backhaul. IEEE Wireless Communications Letters, 2019, 8(2): 552–555.

[16] ALBREEM M A, JUNTTI M, SHAHABUDDIN S. Massive MIMO detection techniques: a survey. IEEE Communications Surveys & Tutorials. 2019, 21(4): 3109–3132.

[17] GAO X, EDFORS O, TUFVESSON F, et al. Massive MIMO in real propagation environments: do all antennas contribute equally? IEEE Trans. on Communications, 2015, 63(11): 3917–3928.

[18] PUGLIELLI A, TOWNLEY A, LACAILLE G, et al. Design of energy- and cost-efficient massive MIMO arrays. Proceedings of the IEEE, 2016, 104(3): 586–606.

[19] ASAAD S, RABIEI A M, MULLER R R. Massive MIMO with antenna selection: fundamental limits and applications. IEEE Trans. on Wireless Communications, 2018, 17(12): 8502–8516.

[20] GAO Y, VINCK H, KAISER T. Massive MIMO antenna selection: switching architectures, capacity bounds, and optimal antenna selection algorithms. IEEE Trans. on Signal Processing, 2018, 66(5): 1346–1360.

[21] TANG H, ZONG X Z, NIE Z P. Global-searching-based iterative swapping antenna selection for massive MIMO systems with imperfect channel estimation. IEEE Access, 2018, 6: 66557–66564.

[22] BENMIMOUNE M, DRIOUCH E, AJIB W, et al. Novel transmit antenna selection strategy for massive MIMO downlink channel. Wireless Networks, 2017, 23: 2473–2484.

[23] GHAZANFARI A, BJORNSON E, LARSSON E G. Optimized power control for massive MIMO with underlaid D2D communications. IEEE Trans. on Communications, 2019, 67(4): 2763–2778.

[24] ZAPPONE A, SANGUINETTI L, BACCI G, et al. Energy-efficient power control: a look at 5G wireless technologies. IEEE Trans. on Signal Processing, 2016, 64(7): 1668–1683.

[25] LIU X X, LI Y Z, XIAO L M, et al. Performance analysis and power control for multi-antenna V2V underlay massive MIMO. IEEE Trans. on Wireless Communications, 2018, 17(7): 4374–4387.

[26] SHEN J C, ZHANG J, ALSUSA E, et al. Compressed CSI acquisition in FDD massive MIMO: how much training is needed? IEEE Trans. on Wireless Communications, 2016, 15(6): 4145–4156.

[27] LIAN L X, LIU A, LAU V K N. Exploiting dynamic sparsity for downlink FDD-massive MIMO channel tracking. IEEE Trans. on Signal Processing, 2019, 67(8): 2007–2021.

[28] KHALILSARAI M B, HAGHIGHATSHOAR S, YI X P, et al. FDD massive MIMO via UL/DL channel covariance extrapolation and active channel sparsification. IEEE Trans. on Wireless Communications, 2019, 18(1): 121–135.

[29] JIAO B L, LIU S J, LEI Y M, et al. A networking solution on uplink channel of co-frequency and co-time system. China Communications, 2016, 13(2): 183–188.

[30] MA M, TIAN S Y, CHEN Y Y, et al. A prototype of co-fre-

quency co-time full duplex networking. IEEE Wireless Communications, 2020, 27(1): 132–139.

[31] KAIMKHANI N A, CHEN Z, YIN F L. Self-interference elimination by physical feedback channel in CCFD for 3-D beamforming communication. China Communications, 2017, 14(9): 62–71.

[32] ZHAO H Z, WANG J, TANG Y X. Performance analysis of RF self-interference cancellation in broadband full duplex systems. Proc. of the IEEE International Conference on Communications Workshops, 2016: 175–179.

[33] XIA X C, XU K, ZHANG D M, et al. Beam-domain full-duplex massive MIMO: realizing co-time co-frequency uplink and downlink transmission in the cellular system. IEEE Trans. on Vehicular Technology, 2017, 66(10): 8845–8862.

[34] LI L X, PETROPULU A P, CHEN Z. MIMO secret communications against an active eavesdropper. IEEE Trans. on Information Forensics and Security, 2017, 12(10): 2387–2401.

[35] GAO H Y, SU Y M, ZHANG S B, et al. Joint antenna selection and power allocation for secure co-time co-frequency full-duplex massive MIMO systems. IEEE Trans. on Vehicular Technology, 2021, 70(1): 655–665.

[36] HUANG Y M, HE S W, WANG J H, et al. Spectral and energy efficiency tradeoff for massive MIMO. IEEE Trans. on Vehicular Technology, 2018, 67(8): 6991–7002.

[37] DAS P P, CHAKRABORTY N, ALLAYEAR S M. Optimal coverage of wireless sensor network using termite colony optimization algorithm. Proc. of the 2nd International Conference on Electrical Engineering and Information Communication Technology, 2015. DOI: 10.1190/ICEEICT.2015.7307523.

[38] GAO H Y, ZHANG S B, SU Y M, et al. Joint resource allocation and power control algorithm for cooperative D2D heterogeneous networks. IEEE Access, 2019, 7: 20632–20643.

[39] XU J, GUO C C, ZHANG H. Joint channel allocation and power control based on PSO for cellular networks with D2D communications. Computer Networks, 2018, 133: 104–119.

[40] WANG S, DA X Y, LI M D, et al. Adaptive backtracking search optimization algorithm with pattern search for numerical optimization. Journal of Systems Engineering and Electronics, 2016, 27(2): 395–406.

Biographies

SU Yumeng was born in 1994. She received her B.S. degree in electronic information engineering from Harbin Engineering University, Harbin, Heilongjiang, China, in 2016. She is currently working toward her Ph.D. degree with Harbin Engineering University. Her current research interests include intelligent computing, resource management, secure communications, massive MIMO, co-frequency co-time full-duplex systems, network slicing, and beyond 5G technologies.
E-mail: suyumeng1994@126.com

GAO Hongyuan was born in 1977. He received his Ph.D. degree from the Department of Communication and Information Systems, College of Information and Communication Engineering, Harbin Engineering University, China, in 2010. He was a visiting research professor with the Department of Computer and Information Science, Korea University, Sejong, South Korea, from 2015 to 2016. He is currently an associate professor with the College of Information and Communication Engineering, Harbin Engineering University. His research interests include wireless energy harvesting communications, intelligent computing, software radio, signal recognition and classification, cognitive radio, array signal processing, long term evolution (LTE)-unlicensed, artificial intelligence, HetNets in 5G, communication theory and image processing, and massive MIMO.
E-mail: gaohongyuan@hrbeu.edu.cn

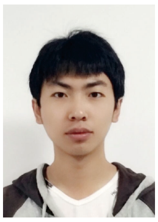

ZHANG Shibo was born in 1994. He received his B.S. degree in electronic information engineering from Harbin Engineering University, Harbin, Heilongjiang, China, in 2016. He is currently working toward his Ph.D. degree with Harbin Engineering University. His research interests include fog/edge computing, cognitive relays, energy harvesting, heterogeneous networks, the Internet-of-Things, and future 6G networks.
E-mail: liangziyanhua@126.com